Journal of Sound and Vibration (2001) **243**(2), 191–213
doi:10.1006/jsvi.2000.3407, available online at http://www.idealibrary.com on IDEAL®

IDENTIFICATION OF COUPLED NON-LINEAR MODES FROM FREE VIBRATION USING TIME-FREQUENCY REPRESENTATIONS

S. Bellizzi, P. Guillemain and R. Kronland-Martinet

Laboratoire de Mécanique et d'Acoustique, CNRS, 31 chemin Joseph Aiguier, 13402 Marseille, France. E-mail: bellizzi@lma.cnrs-mrs.fr

(*Received* 22 *July* 1999, *and in final form* 16 *June* 2000)

A new method based on time–frequency representations is presented for identifying the non-linear modal parameters of a multi-degree-of-freedom non-linear lightly damped mechanical system. The coupled non-linear modes are first introduced. It is shown that, by using the coupled non-linear modes, the free response can be expressed as a linear combination of frequency and amplitude modulated components. This suggests the use of time–frequency methods to characterize these modulation laws and then identify the coupled non-linear modes. These modulation laws are extracted by using an extended definition of the so-called "ridges" of the continuous Gabor transform, which enables a more accurate estimation. An identification procedure of the coupled non-linear modes is proposed and the validity of the whole process is confirmed by performing computer simulations of different types of non-linear elastic dynamic systems.

1. INTRODUCTION

The ability to determine the modal parameters of a mechanical structure is of great interest in structural dynamics, and this is one of the goals of many experimental studies on structural vibrations. In the case of linear structures, the modal theory is a well-known approach to these problems. Classically, based on the principle of superposition, the natural (or normal) modes of vibration of a linear system can be used to express free or forced oscillations. In addition, numerous methods are now available for modal testing analysis [1] and these are commonly used in industrial contexts.

Over the years, many investigations have focussed on the non-linear extension of the definition of the normal mode defined in the classical theory of vibration. In this context, a non-linear normal mode (NNM) of a conservative non-linear discrete or continuous system has been defined as a periodic oscillation where all the material points in the system reach their extreme value or pass through zero simultaneously. The concept of NNM has been introduced by Rosenberg [2] for a system with n masses interconnected by strongly non-linear springs. More recently, an interesting approach in terms of invariant manifolds was proposed by Shaw and Pierre [3, 4]. These authors define an NNM as a motion which takes place on a two-dimensional invariant manifold in the phase space. These approaches have been used in many subsequent efforts to construct the NNM of conservative non-linear systems, which would provide a valuable tool for understanding some essentially non-linear dynamic phenomena (see the recent review by Vakakis [5]).

As in the case of linear theory, the NNM are associated with a particular set of initial conditions, and since the superimposition principle is not valid in the non-linear case, the

0022-460X/01/220191 + 23 $35.00/0

NNM cannot be used directly to express the response under arbitrary initial conditions. To overcome this difficulty, several approaches have been proposed. Shaw and Pierre [3] have used "a non-linear co-ordinate transformation which performs the same function as the well-known linear modal transformation in that it allows one to assemble a complete solution from a sum of simpler (the NNM) ones". Szemplinska-Stupnicka [6] introduced the concept of coupled non-linear modes (CNMs). The free oscillations (with arbitrary initial conditions) of a conservative non-linear system are approximated by a linear combination of harmonic terms. Each harmonic term depends on a mode shape vector and its corresponding frequency. Each couple of a frequency and a mode shape vector defines a CNM. One important aspect of the CNMs is that the frequencies and mode shapes depend on the amplitude of all the modes, whereas each NNM depends only on its amplitude. The concept of the CNMs was also developed by Bellizzi and Bouc [7, 8] to analyze lightly damped mechanical systems with strongly non-linear restoring forces under random input.

Since the CNMs provide a valuable tool for characterizing a mechanical system with non-linear restoring forces, an important question arises: how to identify the CNMs from measured data? This inverse problem is addressed in this paper. A method for identifying the CNMs of a multi-degree-of-freedom (m.d.o.f.) lightly damped mechanical system with strongly restoring forces from transient response is presented. First, based on the generalized van der Pol transformation, the CNMs are used to express the transient response as a linear combination of quasi-harmonic terms giving a quasi-modal constitutive behaviour. Each quasi-harmonic term characterizes the contribution of each CNM as the product of three functions of time, namely the instantaneous (modal) amplitude, the instantaneous frequency and the mode-shape vector. As mentioned above, the mode-shape vector functions and the instantaneous frequency functions are amplitude dependent. The expression of the quasi-harmonic terms in terms of sinusoids modulated both in amplitude and frequency suggests the use of time–frequency analysis [9] to extract the modulation laws. Time–frequency analysis has been previously applied to estimate the modal parameters of a vibrating linear system [10, 11]. Time–frequency analysis has also been used in the context of non-linear system identification as a tool to detect [12] or to classify [13] the non-linearity. In reference [12], the proposed technique is based on joint application of Gabor and Hilbert transforms but methods only based on the Hilbert transform have also been developed [14]. More recently, an identification procedure for m.d.o.f. non-linear systems based on (multi-scale) ridges and skeletons of the wavelet transform was proposed in reference [15]. It is important to underline that, in general the systems identified by these approaches, with the exception of the one-degree-of-freedom case, do not constitute the physical model of the system. The method used in the paper is based on an extended definition of the "ridges" of the continuous time–frequency representations which have not been used yet in the context of the analysis of non-linear vibrations. The method requires the use of a frequency modulated analyzing function and involves the partial derivatives of the phase of the transform with respect to both the time and the frequency. Moreover, the interest of our approach is that by focusing on the CNMs, we have a tool for identifying the physical model of the system.

This paper is organized as follows. In section 2, the mechanical system under investigation is presented. The CNMs are formulated and used in the van der Pol transformation to express the free response of the system. In section 3, the concept of time–frequency analysis is briefly introduced. We then present the new definition of the "ridges" of the continuous Gabor transform, and show how it can be used to estimate the modulation laws. Finally, an identification procedure of the CNMs is given. In section 4, three numerical experiments are described to illustrate the whole process.

2. COUPLED NON-LINEAR MODES AND TRANSIENT RESPONSE

2.1. MECHANICAL SYSTEM UNDER STUDY

Consider an n d.o.f. autonomous mechanical system governed by the differential equations

$$[M]\ddot{X}(t) + 2\xi[C]\dot{X}(t) + F(X(t)) = \mathbf{0}, \quad t \in [0, T], \tag{1}$$

$$X(0) = X^0, \quad \dot{X}(0) = \dot{X}^0, \tag{2}$$

where the dot denotes the derivative with respect to time, $X(t) = (X_1(t), \ldots, X_n(t))^{\mathrm{T}}$ is the displacement vector, $[M]$ and $2\xi[C]$ are the inertia and damping matrices (ξ is a real positive parameter), the vector function F ($\mathbb{R}^n \mapsto \mathbb{R}^n$) gives the stiffness forces acting on the system, and $X^0 \in \mathbb{R}^n$ and $\dot{X}^0 \in \mathbb{R}^n$ denote the initial conditions. F is required to be a monotonic piecewise continuously differentiable vector function, $[M]$ and $[C]$ to be symmetric, positive-defined matrices and ξ to be strictly positive, and arbitrarily small ($0 < \xi \ll 1$). The last assumption means that the study is restricted to a lightly damped mechanical system. It is also assumed that there exists a single root, $X^e \in \mathbb{R}^n$, of $F(X^e) = 0$ and that the linearized system obtained by linearizing (1) about the equilibrium point X^e has n natural modes (i.e., $[\partial F(X^e)]\psi^e = \omega^{e^2}\psi^e$ where $[\partial F(X)]$ denotes the Jacobian matrix) with n distinct and incommensurable natural frequencies. Note that it is not assumed that $F(-X) = -F(X)$.

This class of mechanical systems has been studied in references [7, 8] under additive random excitation. A stochastic linearization method with random matrices was proposed to characterize the stationary response. This method is based on decomposing the stationary response dynamics. The same formalism will be used here to relate the transient response to the CNMs. We shall begin by introducing the notion of coupled non-linear modes.

2.2. COUPLED NON-LINEAR MODES

Consider the autonomous conservative system associated with (1),

$$[M]\ddot{X}(t) + F(X(t)) = 0. \tag{3}$$

The coupled non-linear modes are defined from a multi-harmonic approximation based on the harmonic balance method to the solution of equations (2) and (3),

$$X(t) = \Psi_0 + \sum_{i=1}^{n} \Psi_i a_i \cos(\Omega_i t + \varphi_i), \tag{4}$$

$$\Psi_i^{\mathrm{T}}[M]\Psi_i = 1, \text{ for } i = 1, \ldots, n, \tag{5}$$

where the vector $\Psi_0 \in \mathbb{R}^n$ defines the position or offset, around which the movement is established, the frequency-mode shape $(\Omega_i, \Psi_i) \in \mathbb{R}_+ \times \mathbb{R}^n$ couples denote n non-linear modes, and $a_i > 0$ and $\varphi_i \in [0, 2\pi]$ are constants depending on X^0 and $\dot{X}^0$. Due to the normalization property (5), a_i defines the modal amplitude of the ith coupled non-linear mode.

Substituting expression (4) into equation (3) and applying the harmonic balance procedure yields the non-linear algebraic equations

$$\mathscr{F}_0(a; \Psi) = 0, \tag{6}$$

$$\frac{1}{a_i}\mathscr{F}_i(a;\Psi) = [M]\Psi_i\Omega_i^2, \quad \text{for } i = 1,\dots,n, \tag{7}$$

$$\Psi_i^{\mathrm{T}}[M]\Psi_i = 1, \quad \text{for } i = 1,\dots,n, \tag{8}$$

where

$$\mathscr{F}_0(a;\Psi) = \int_\phi F\left(\Psi_0 + \sum_{m=1}^{n}\Psi_m a_m\cos\phi_m\right)\mathrm{d}\phi, \tag{9}$$

$$\mathscr{F}_i(a;\Psi) = 2\int_\phi F\left(\Psi_0 + \sum_{m=1}^{n}\Psi_m a_m\cos\phi_m\right)\cos\phi_i\,\mathrm{d}\phi, \tag{10}$$

with $a = (a_1,\dots,a_n)$, $\Psi = (\Psi_0, \Psi_1,\dots,\Psi_n)$ and the notation

$$\int_\phi(\cdot)\,\mathrm{d}\phi = \frac{1}{(2\pi)^n}\int_0^{2\pi}\cdots\int_0^{2\pi}(\cdot)\,\mathrm{d}\phi_1\dots\mathrm{d}\phi_n. \tag{11}$$

Solving, for fixed $a\in\mathbb{R}^n$, the non-linear equations (6)–(8), with respect to the $n + n^2 + n$ unknowns Ψ_0, Ψ_i and Ω_i yields the coupled non-linear modes as a function of the amplitude vector a:

$$\Psi_0 \equiv \Psi_0(a), \quad \Omega_i \equiv \Omega_i(a), \quad \Psi_i \equiv \Psi_i(a), \qquad \text{for } i = 1,\dots,n. \tag{12}$$

The function Ω_i (respectively, the vector function Ψ_i) characterizes the evolution of the frequency (respectively, the mode shape) versus the amplitude vector a. For $n = 1$, $\Psi_i = 1$ and the function $\Omega(a)$ represents the inverse backbone curve of the system. The reader is referred to reference [7] for a discussion about its existence and uniqueness.

The normalization of the vector mode shapes has been defined in equation (5). Nevertheless, it should be pointed out that this normalization procedure is not the only possible one, and other definitions can be used, (for example, $\Psi_{ii} = 1$). As regards the property of orthogonality, since no hypothesis as to the symmetry is made on the Jacobian matrix of F, the vector mode shapes $\Psi_i(a)$ for $i = 1,\dots,n$ do not generally comply with the orthogonality properties. It is then usual to associate with the modal matrix $[\Psi(a)] = [\Psi_1(a)\cdots\Psi_n(a)]$ the adjoint modal matrix denoted $[\Gamma(a)]$, which is classically defined by

$$[\Gamma(a)]^{\mathrm{T}}[M][\Psi(a)] = [I], \tag{13}$$

where $[I]$ denotes the identity matrix.

Note that the CNMs give a harmonic approximation of the NNMs when the procedure is applied with $a = (0,\dots,0,a_i,0,\dots,0)$ and $a_i \neq 0$. Hence the solution of the conservative system with arbitrary initial conditions is not defined as a linear combination of the NNM, and this is in agreement with the principle of superposition, which is not valid in the case of non-linear systems.

2.3. FREE OSCILLATIONS FOR THE DAMPED SYSTEM

The aim of this section is to express the transient response of the damped system (1, 2) from the CNM functions. For this purpose, the averaging principle is used.

Consider the amplitude-phase transformation

$$X(t) = \Psi_0(a(t)) + \sum_{i=1}^{n} \Psi_i(a(t)) a_i(t) \cos \phi_i(t), \tag{14}$$

$$\dot{X}(t) = -\sum_{i=1}^{n} \Psi_i(a(t)) \Omega_i(a(t)) a_i(t) \sin \phi_i(t), \tag{15}$$

$$\phi_i(t) = \theta_i(t) + \varphi_i(t) = \int_0^t \Omega_i(a(s))\, \mathrm{d}s + \varphi_i(t) \quad \text{for } i = 1, \ldots, n, \tag{16}$$

where Ψ_0, Ω_i and Ψ_i denote the CNM, $a_i(t) > 0$ (respectively, $\varphi_i(t) \in [0, 2\pi]$) defines the modal amplitude (respectively, the associated phase) of the ith CNM. Equation (14) is similar to equation (4), but due to the dissipative terms, the amplitude and phase vectors are now taken to be functions of time and the $\theta_i(t)$ terms have been formulated in order to take into account the change in the instantaneous frequencies.

Upon using equations (14)–(16) the equations of motion (1, 2) take the forms

$$\dot{a}(t) = \xi f(a(t), \theta(t) + \varphi(t)), \tag{17}$$

$$\dot{\varphi}(t) = \xi g(a(t), \theta(t) + \varphi(t)), \tag{18}$$

$$\dot{\theta}(t) = \Omega(a(t)), \tag{19}$$

where f and g are multi-periodic vector functions with respect to the second variable $\theta + \varphi$ (the total phase). In general, these differential equations are as difficult to solve as the original ones. Nevertheless, for a small ξ (which is the case here), a and φ are slowly varying functions with respect to the variation of X and it is possible to obtain an approximate solution by using the averaging principle [16] based on the mean operator (11). As described in reference [7] and based on some simplifying additional hypothesis, the differential system (17)–(19) can be replaced by the averaged differential equations

$$\begin{cases} \dot{a}_i(t) = -\xi \dfrac{c_i(a(t))}{\bar{D}_i(a(t))} a_i(t) \\ a_i(0) = a_i^0 \end{cases} \quad \begin{cases} \dot{\varphi}_i(t) = 0 \\ \varphi_i(0) = \varphi_i^0 \end{cases} \quad \text{for } i = 1, \ldots, n, \tag{20}$$

where the initial conditions a_i^0, φ_i^0 are constants depending on X^0 and $\dot{X}^0$,

$$c_i(a) = \Gamma_i^{\mathrm{T}}(a)[C]\Psi_i(a) \quad \text{and} \quad \bar{D}_i(a) = 1 + \frac{a_i}{2\Omega_i(a)} \frac{\partial \Omega_i(a)}{\partial a_i} + \Gamma_i^{\mathrm{T}}(a)[M] \frac{\partial \Psi_i(a)}{\partial a_i} a_i. \tag{21}$$

In the averaging approximation sense, the displacement vector takes the form

$$X(t) = \Psi_0(a(t)) + \sum_{i=1}^{n} \Psi_i(a(t)) a_i(t) \cos\left(\int_0^t \Omega_i(a(s))\, \mathrm{d}s + \varphi_i^0 \right), \tag{22}$$

where the amplitude vector function a and the phase vector function φ solve the differential equations (20). The vector function φ is a constant vector function (equal to φ^0) which depends only on the initial conditions X^0 and $\dot{X}^0$. The n differential equations characterizing the n modal amplitude components a_i are coupled. The logarithmic derivative of a_i with respect to time is strongly influenced by the damping matrix $\xi[C]$. Note that as in the linear case, this expression is valid only for lightly damped mechanical

systems because it does not take into account the frequency shift introduced by the damping.

The expression (22) can be viewed as the result of the direct problem and we will now focus on the inverse problem consisting of identifying the CNMs from the time history of the transient response.

3. TIME–FREQUENCY REPRESENTATION AND NON-LINEAR VIBRATIONS

In the previous sections, it has been shown that non-linear systems give rise to vibrations that can be decomposed into a sum of simple elements. These simple elements consist of quasi-monochromatic signals the amplitude and frequency of which are both modulated, as expressed by equation (22). In this section, we address the problem of characterizing non-linear vibrations by extracting the corresponding modulation laws for each simple element. From the practical point of view, this problem can be said to constitute a signal processing problem. Actually, the aim is to decompose a given signal into the so-called spectral lines, which are monochromatic signals, the frequency and amplitude of which are both modulated [17]. Consider a scalar signal $s(t)$ which is a combination of these simple elements

$$s(t) = \sum_{i=1}^{n} A_i(t) \cos \Phi_i(t). \tag{23}$$

Characterizing $s(t)$ requires a description which provides information about its behaviour in both the time and frequency domains. Although time and frequency are dual representations with respect to the Fourier transform, one looks for a joint representation with which the process of analysis can be easily interpreted. Actually, the time behaviour of the energy as well as the variations of the instantaneous frequency of a signal are known to be "hidden" in the phase and the modulus of its Fourier transform. In the general case, where no *a priori* knowledge on the signal can be used, a frequency representation does not give easily extractable modulation laws. Conversely, we shall describe how time–frequency representations of non-stationary signals can be used to extract from signals of this kind the functions $A_i(t)$ and $\Phi_i'(t)$ (or $\Phi_i(t)$), yielding practical tools for characterizing nonlinear vibrations. In this section, the prime will denote the derivative with respect to time.

3.1. TIME–FREQUENCY REPRESENTATIONS OF NON-STATIONARY SIGNALS

Describing the distribution of the energy of an arbitrary signal on a time–frequency plane is very important when it comes to addressing the analysis of evolving signals. This problem can arise in many fields, including the study of mechanical vibrations, such as for example those arising in non-destructive evaluation problems or the characterization of audiophonic signals. The problem can be expressed as follows: consider a signal $s(t)$ with a finite energy E; is it possible to find an energy density $\rho(t, \omega)$ such that E is "spread out" over the time–frequency plane?:

$$E = \int\int \rho(t, \omega)\, \mathrm{d}\mu(t, \omega). \tag{24}$$

We shall not discuss here the general classes of solutions to this problem. Since the signals we consider are multi-component signals, we shall focus on linear time–frequency

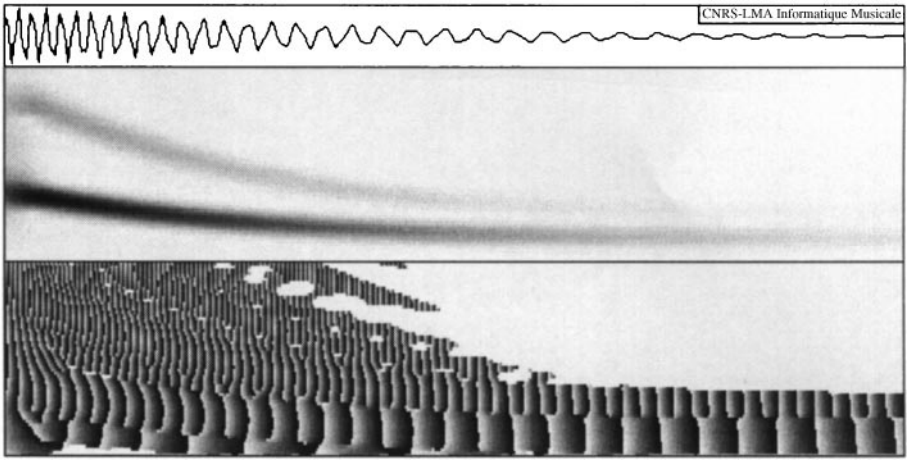

Figure 1. Signal analyzed (free oscillation, component x_1 of Example 1), modulus and phase of the Gabor transform.

representations in order to avoid interference terms in the representation. More particularly, we shall use the continuous Gabor transform [18].

The Gabor transform of a signal $s(t)$ with respect to the window $W(t)$ is given by

$$L_g(\tau, \alpha) = \int s(t)\,\bar{W}(t-\tau)\,\mathrm{e}^{-\mathrm{j}\alpha(t-\tau)}\,\mathrm{d}t. \tag{25}$$

The correspondence $s \to L$ is linear, invertible and covariant by translation in both time and frequency.

Other linear representations can be used, such as the wavelet transform, which is defined by reference [9] as

$$T(b, a) = \frac{1}{a}\int \bar{g}\left(\frac{t-b}{a}\right) s(t)\,\mathrm{d}t. \tag{26}$$

The choice of one or the other representation depends on the problem being addressed. The wavelet transform is well adapted to transient signals (covariance by change of scale), while the Gabor transform is suitable for quasi-periodic signals. In what follows, we shall describe how the Gabor transform can be used to characterize non-linear vibrations, but all the methods described can be transposed to the wavelet transform. In the next section, we describe methods based on the time–frequency representations to accurately extract each non-linear mode.

3.2. EXTRACTION OF FREQUENCY AND AMPLITUDE MODULATION LAWS OF A SIMPLE ELEMENT OF A SIGNAL

Linear time–frequency representations such as Gabor representations are obtained by comparing the signal in the vicinity of a given time with a family of analyzing functions. The values obtained in this way are redundant, and only a subset of them are relevant in terms of the information they convey. This assumption can be expressed mathematically by the fact that the transforms are defined within a Hilbert space with reproducing kernel [19]. The

question which naturally arises is then as follows: is it possible to extract from a time–frequency representation a set of values such that all the information is preserved? As we shall see, this set of values defines the so-called ridge of the transform. This ridge corresponds to trajectories in the time–frequency plane following the frequency modulation law of each simple element and allowing a precise description of each of them. Here we shall present a formulation for analyzing mechanical vibrations based on an extension of the classical "ridges" approach. The reader is referred to reference [20] for further details and other applications of the method.

Consider a non-stationary asymptotic signal $s(t) = A_s(t)\mathrm{e}^{\mathrm{j}\Phi_s(t)}$ and assume that its frequency modulation law is locally linear and that its amplitude modulation law can be expressed locally by a polynomial

$$\Phi_s(t) \simeq \Phi_s(\tau) + (t-\tau)\,\Phi_s'(\tau) + \frac{1}{2}(t-\tau)^2\,\Phi_s''(\tau), \tag{27}$$

$$A_s(t) = \sum_{k=0}^{k=\infty} \frac{(t-\tau)^k}{k!}\,A_s^{(k)}(\tau). \tag{28}$$

Consider now a "chirped window" $W(t)$, which will be used to select parts of the signal:

$$W(t) = \exp\left(\frac{-t^2}{2\sigma^2}\right)\exp\left(\mathrm{j}\beta\frac{t^2}{2}\right). \tag{29}$$

The Gabor transform of $s(t)$ is given by

$$L_g(\tau,\alpha) \simeq \exp(\mathrm{j}\Phi_s(\tau))\,\sigma\sqrt{\frac{2\pi}{1-\mathrm{j}\sigma^2(\Phi_s''(\tau)-\beta)}} \times \sum_{k=0}^{k=\infty}\frac{(\mathrm{j})^k}{k!}\,A_s^{(k)}(\tau)\,\frac{\partial^k}{\partial\alpha^k}\exp\left(-\frac{\sigma^2}{2}\frac{(\Phi_s'(\tau)-\alpha)^2}{1-\mathrm{j}\sigma^2(\Phi_s''(\tau)-\beta)}\right). \tag{30}$$

Since the signal is asymptotic, one can assume that the term of order $k=0$ in the above series is predominant. Consequently, the transform is mainly governed by the term

$$A_s(\tau)\exp\left(-\frac{\sigma^2}{2}\frac{(\Phi_s'(\tau)-\alpha)^2}{1-\mathrm{j}\sigma^2(\Phi_s''(\tau)-\beta)}\right) \simeq A_s(\tau)\,\hat{W}(\Phi_s'(\tau)-\alpha)^{1/(1-\mathrm{j}\sigma^2(\Phi_s''(\tau)-\beta))}. \tag{31}$$

The behaviour of the transform can then be interpreted as a set of superimposed Fourier transforms of $W(t)$ located along the curve $\Phi_s'(\tau)=\alpha$, called the ridge, that describes the frequency modulation law of the signal in the $\{\tau,\alpha\}$ plane (see Figure 2 of section 4).

In order to extract the frequency modulation law of the signal, one has to estimate the curve $\Phi_s'(\tau)=\alpha$ with the help of the coefficients of the transform. If the second derivative of the phase of the analyzing function fits the second derivative of the phase of the signal ($\Phi_s''(\tau)=\beta$) the transform is given by

$$L_g(\tau,\alpha) = \exp(\mathrm{j}\Phi_s(\tau))\,\sigma\sqrt{2\pi}\sum_{k=0}^{\infty}\frac{(\mathrm{j})^k}{k!}\,A_s^{(k)}(\tau)\,\frac{\partial^k}{\partial\alpha^k}\exp\left(-\frac{\sigma^2}{2}(\Phi_s'(\tau)-\alpha)^2\right) \tag{32}$$

With $\Phi_g(\tau,\alpha)$ denoting the phase of the Gabor transform, one can then show that the ridge of the transform given by $\Phi_s'(\tau)=\alpha$ and $\Phi_s''(\tau)=\beta$ corresponds to the set of points on the

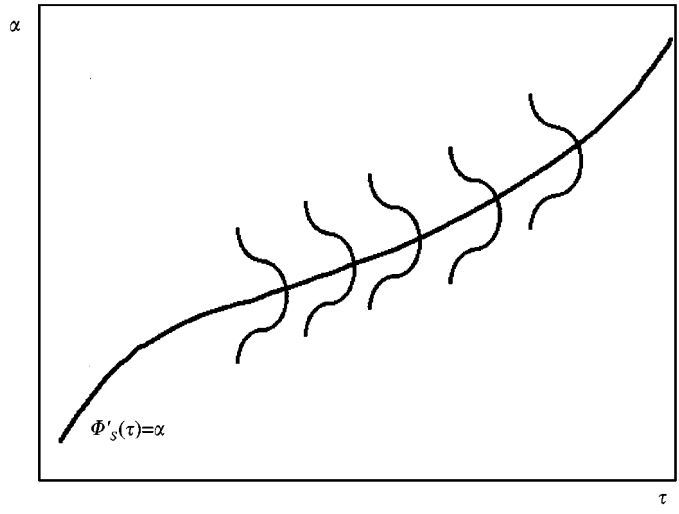

Figure 2. Behaviour of the Gabor transform of a time-asymptotic signal as a superimposition of $\hat{W}$.

time–frequency plane satisfying the so-called crossed criterion [20]

$$\left(\frac{\partial}{\partial\tau} + \Phi_s''(\tau)\frac{\partial}{\partial\alpha}\right)\Phi_g(\tau, \alpha) = \Phi_s'(\tau) = \alpha, \tag{33}$$

$$\left(\frac{\partial}{\partial\tau} + \Phi_s''(\tau)\frac{\partial}{\partial\alpha}\right)^2 \Phi_g(\tau, \alpha) = \Phi_s''(\tau) = \beta. \tag{34}$$

This criterion allows the signal to be "viewed" through an adaptive filter which adjusts itself to the variations with time in the frequency of each simple element and whose frequency modulation automatically adapts to that of the signal by matching both the frequency modulation law and its slope. Moreover, since $\exp(-(\sigma^2/2)(\Phi_s'(\tau) - \alpha)^2)$ is symmetric with respect to the curve $\Phi_s'(\tau) = \alpha$, on the ridge, its odd order derivatives are zero. Consequently, the series in equation (32) is real and the phase of the transform along the ridge exactly matches the phase of the signal,

$$\Phi_s(\tau) = \Phi_g(\tau, \Phi_s'(\tau)) \tag{35}$$

and the amplitude modulation law of the signal is approximated by the modulus of the transform along the ridge:

$$A_s(\tau) \simeq \frac{1}{\sqrt{2\pi}\sigma}\,|L_g(\tau, \Phi_g'(\tau))|. \tag{36}$$

In the context of this study, signals possess several simple elements. This might seem to be a limitation restricting the use of this method, which has been discussed only in the case of a single simple element. Nevertheless, in practice, it is usually possible to choose a frequency selectivity that makes it possible to separate the components. Locally, the Gabor analysis therefore deals only with one component. The bandwidth of the Gaussian analyzing window used can be tuned to avoid any interferences from the other components by suitably adapting its parameter σ. This problem is discussed in Appendix and a procedure is proposed to extract the modulation laws.

3.3. COMPARISON WITH OTHER TECHNIQUES

In this section, we shall compare this method of estimation of modulation laws with other techniques using also continuous linear time–frequency and time-scale representations. We shall mainly consider the techniques previously used in the framework of identification of non-linear modes.

Generally speaking, the redundancy of the continuous linear joint representations brings up the problem of identification of trajectories in the domain of definition of the transforms carrying a "relevant" information, in the sense that the restrictions of the transforms along these trajectories allows the most accurate reconstruction of the signal. Several solutions to this problem have been proposed. They all lead to criteria involving the partial derivatives of the phase and the modulus of the representations and are based on approximations of the transforms [21] using the stationary phase approximation technique. We shall first consider a single simple element signal and summarize the performances and limitations of these methods, ending with a comparison with the method we propose.

- Ridges and skeletons of the continuous wavelet transform. In the case of an asymptotic signal (i.e., the amplitude of which varies slowly with respect to the phase), it can be shown [21] that the ridge of the transform leads to an exact estimate of the frequency modulation law only when the amplitude of the signal is constant and its frequency modulation law is linear. When these conditions are not met, there exists a bias, depending both on the bandwidth of the wavelet and on the derivatives of the amplitude and frequency modulation laws. Without any approximation, it can be shown also [20] that the wavelet transform provides an exact estimate of frequency modulation laws of hyperbolic type, corresponding to homogeneous functions with complex degree.
- Ridges and skeletons of the continuous Gabor transform. When using the same formalism and approximations as in the wavelet case, the conclusions are the same. The different geometry of the time–frequency plane with respect to the time-scale half-plane does not yield any sympathetic properties in the case of signals with hyperbolic frequency modulation laws.
- Ridge of the Gabor transform using an adaptive window (our case). The choice of an adapted window, the frequency modulation of which automatically matches the frequency modulation law of the signal along the ridge lets one relax the constant amplitude modulation law or the linear frequency modulation law assumptions. The exact estimation of a linear frequency modulation law is possible whatever the amplitude modulation law. It can also be shown that an exact estimation of a parabolic frequency modulation law with a constant amplitude modulation law is possible.

In the case of signals with several simple elements, the advantage of our method resides in its ability to separate simple elements the distance of which is small in the time frequency plane. This is an important point in our context. We shall briefly discuss the classical case of two "parallel" linear frequency modulated components by considering the spreading of the time–frequency atoms (reproducing kernels) along the ridges in the wavelet case, in the Gabor case and in our adaptive Gabor case. Figure 3 of section 4 shows the reproducing kernels corresponding to a wavelet analysis, a Gabor analysis, an adaptive Gabor analysis of a signal composed of a sum of two parallel linear frequency modulated simple elements. The horizontal axis is the time. The vertical axis is the frequency. The exact frequency modulation laws are represented by the two parallel straight lines. From left to right one can see the following.

- Reproducing kernel of a small-scale wavelet analysis or a wide-band Gabor analysis (σ small, $\beta = 0$). In this case, the transform shows beats coming from the interferences between the two simple elements of the signal in the frequency domain.

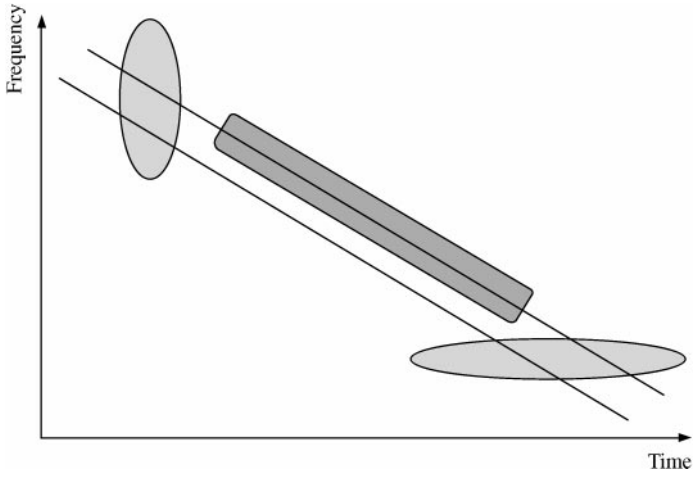

Figure 3. Reproducing kernel for different time–frequency representations (from left to right, Gabor analysis with σ small and $\beta = 0$, matched Gabor analysis with σ large and $\beta \neq 0$, Gabor analysis with σ large and $\beta = 0$).

- Reproducing kernel of a Gabor analysis using a matched window the frequency modulation of which follows on that of the signal ($\beta \neq 0$). In this case, it is possible to increase the selectivity of the analysis through the use of a large σ to allow a better separation of the simple elements.
- Reproducing kernel of a large-scale wavelet analysis or a narrow-band Gabor analysis (σ large, $\beta = 0$). In this case, the transform shows beats coming from the interferences between the two simple elements on the signal in the time domain.

3.4. IDENTIFICATION OF COUPLED NON-LINEAR MODES

As has been established in section 2, the transient response of system (1, 2) is given by equation (22) and can be rewritten component by component as

$$X_m(t) = \Psi_{m0}(t) + \sum_{i=1}^{n} A_{mi}(t) \cos \phi_i(t), \quad m = 1, \ldots, n, \tag{37}$$

where

$$A_{mi}(t) = \Psi_{mi}(a(t))a_i(t) \quad \text{and} \quad \phi_i(t) = \int_0^t \Omega_i(a(s))\, \mathrm{d}s + \varphi_i^0. \tag{38}$$

Each component $X_m(t)$ consists of a sum of quasi-harmonic terms (or simple elements with the terminology used in section 3) with amplitudes, $A_{mi}(t)$, and instantaneous frequencies, $\Omega_i(a(t))$ varying slowly with respect to time. The term $A_{mi}(t) \cos \phi_i(t)$ corresponds to the contribution of the ith CNM to the jth component of $X(t)$.

From a time history of the transient response sampled with a time-step Δt, $X(t_k) = X(k\Delta t)$, for $k = 1, \ldots, N$, the proposed procedure to identify the CNMs comprises two steps.

Step 1. For each component X_m, the amplitude $A_{mi}(t_k)$, the instantaneous frequency $\Omega_i(a(t_k))$ and phase $\phi_i(t_k)$ (for $k = 1, \ldots, N$) of each simple element are extracted using the procedure described in the Appendix A. The estimates are denoted $\tilde{A}_{mi}(t_k)$, $\tilde{\Omega}_{mi}(t_k)$ and $\tilde{\phi}_{mi}(t_k)$, respectively. Note that the function Ψ_{m0} can be estimated by performing a simple

low pass filtering procedure that removes all the other CNMs. This filtering procedure naturally involves considering the restriction of the Gabor transform for $\alpha = 0$.

Step 2. From equation (38), the modal amplitudes a_i and the mode shapes $\Psi_i(a)$ are estimated by using the following formulae:

For $k = 1, \ldots, N$, for $i = 1, \ldots, n$

$$\tilde{a}_i(t_k) = \tilde{A}_{ii}(t_k),$$

$$\tilde{\Psi}_{ii}(\tilde{a}(t_k)) = 1,$$

$$\tilde{\Psi}_{mi}(\tilde{a}(t_k)) = \begin{cases} \dfrac{\tilde{A}_{mi}(t_k)}{\tilde{A}_{ii}(t_k)} & \text{if } |\tilde{\phi}_{mi}(t_k) - \tilde{\phi}_{ii}(t_k)| \geqslant \pi \\ -\dfrac{\tilde{A}_{mi}(t_k)}{\tilde{A}_{ii}(t_k)} & \text{if } |\tilde{\phi}_{mi}(t_k) - \tilde{\phi}_{ii}(t_k)| < \pi \end{cases} \quad \text{for } m = 1, \ldots, n, m \neq i.$$

where the tilde denotes the estimate.

Hence, this procedure leads to an estimate for the CNMs on the subset $\mathscr{A} = \{(\tilde{a}_1(t_k), \ldots, \tilde{a}_n(t_k)) \in \mathbb{R}_+^n / k = 1, \ldots, N\}$ as

$$a \in \mathscr{A} \to \begin{cases} \Psi_0(a) \\ (\tilde{\Omega}_i(a), \quad \tilde{\Psi}_i(a)) \quad \text{for } i = 1, \ldots, n. \end{cases} \tag{39}$$

The subset $\mathscr{A}$ corresponds to the trajectory of the measured data in the "modal amplitude space".

Some remarks can be made on the above procedure.

The sign of the mode shape components is obtained by using the phase behaviour.

The analysis of a given component does not generally make it possible to estimate all the modes. Actually, the contribution of some modes can be very slight, depending on the measurement point location. In addition, depending on the initial conditions, some modes are sometimes not excited.

There is redundant information for estimating the modal frequencies. Actually, each component gives these frequencies. Nevertheless, this redundancy can be useful and can help to improve the results, for example by correcting the biased ridges on some components.

4. NUMERICAL RESULTS

In this section, we give some computer simulation results. The estimated coupled non-linear modes are compared with the theoretical ones in the case of three different non-linear systems. The free responses are obtained by solving the non-linear differential system (1, 2) numerically, by using the Newmark scheme. The estimated coupled non-linear modes are obtained with the method described above. For this purpose, the value of σ was chosen such that it gives a suitable frequency separation in the time–frequency plane. The theoretical coupled non-linear modes are obtained by solving (analytically or numerically) the non-linear algebraic system (6–8) by using the Newton–Raphson method for each estimated modal amplitude vector.

4.1. SYSTEMS WITH TWO DOF AND CUBIC NON-LINEARITY

Consider the mechanical system (1, 2) with $n = 2$, $[C] = [I]$ and $F(X) = [K_0]X + (X^T[K_1]X)[K_1]X$ where $[K_0]$ and $[K_1]$ are two real matrices. Two cases have been studied, one of which yields expressions for the theoretical coupled non-linear modes with

amplitude-independent mode shapes. In each case, the $[M]$-normalization procedure was used to define the mode shapes.

4.1.1. *Example* 1

Here the system studied is defined by $[K_1] = \lambda[K_0]$ where λ is a non-negative constant. One can easily check that the coupled non-linear modes are

$$\Omega_1^2(a_1, a_2) = \bar{\omega}_1^2\left(1 + \frac{3}{4}\lambda^2 a_1^2\bar{\omega}_1^2 + \frac{1}{2}\lambda^2 a_2^2\bar{\omega}_2^2\right), \quad \Psi_1(a_1, a_2) = \bar{\Psi}_1, \tag{40}$$

$$\Omega_2^2(a_1, a_2) = \bar{\omega}_2^2\left(1 + \frac{1}{2}\lambda^2 a_1^2\bar{\omega}_1^2 + \frac{3}{4}\lambda^2 a_2^2\bar{\omega}_2^2\right), \quad \Psi_2(a_1, a_2) = \bar{\Psi}_2, \tag{41}$$

where $(\bar{\omega}_k^2, \bar{\Psi}_k)$ for $k = 1, 2$ correspond to the natural modes of the undamped linear system defined by $\lambda = 0$: i.e.,

$$[K_0]\,\bar{\Psi}_k = \bar{\omega}_k^2[M]\,\bar{\Psi}_k, \quad \bar{\Psi}_k^{\mathrm{T}}[M]\,\bar{\Psi}_k = 1. \tag{42}$$

Figure 4 shows the free response obtained with $\xi = 0{\cdot}02$, $\lambda = 3$,

$$[M] = \begin{pmatrix} 1 & 0{\cdot}5 \\ 0{\cdot}5 & 1 \end{pmatrix}, \quad [K_0] = \begin{pmatrix} 1 & 1 \\ 1 & 4 \end{pmatrix}, \quad X^0 = \begin{pmatrix} 0{\cdot}5 \\ 0{\cdot}5 \end{pmatrix}, \quad \dot{X}^0 = \begin{pmatrix} 0 \\ 0 \end{pmatrix}$$

used as the input data for the proposed method. Figure 1 gives the modulus and the phase of the Gabor transform of the first component (shown on the top). The horizontal axis is the

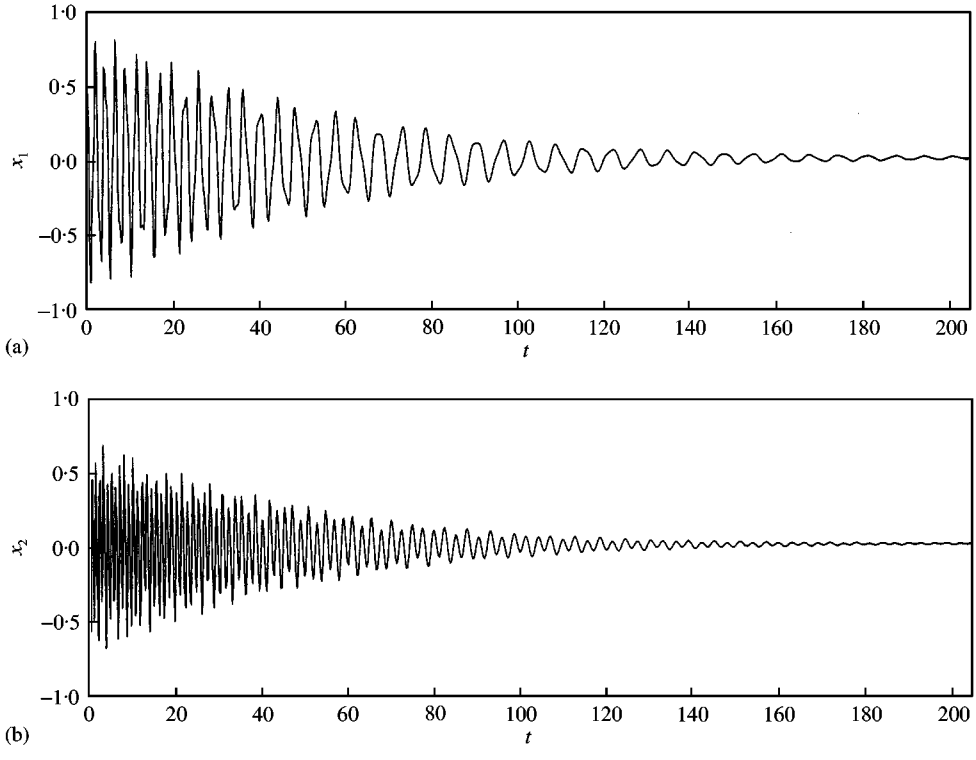

Figure 4. Example 1. Free oscillation.

time, and the vertical axis, the frequency. The values of the representation are coded according to a grey-scale palette. One can see two nearly horizontal stripes corresponding to non-linear modes. Figure 5 (top curves) shows the changes with respect to time in the modal amplitudes ($a_1(t)$ and $a_2(t)$) extracted by time–frequency analysis. These amplitudes have been used to calculate the theoretical coupled non-linear modes. Figure 5 shows the theoretical and extracted frequency modulation laws governing the two modes. Figure 6 compares the evolution of the theoretical and extracted mode shapes with respect to time. As expected, these mode shapes do not depend on time. Good agreement can be seen to exist between the theoretical and extracted curves. Note also, for each mode, that there exists good agreement between the extracted frequencies obtained from each component. A bias can, nevertheless, be observed at the beginning of the curves, due to the presence of a singularity (the signal is assumed to be zero for negative values of time) detected by the time–frequency analysis process.

4.1.2. *Example* 2

Consider now the system defined by $\xi = 0{\cdot}02$, $\lambda = 1$,

$$[M] = \begin{pmatrix} 1 & 0{\cdot}7 \\ 0{\cdot}7 & 1 \end{pmatrix}, \quad [K_0] = \begin{pmatrix} 1 & 1 \\ 1 & 6 \end{pmatrix}, \quad [K_1] = \begin{pmatrix} 3 & 2 \\ 2 & 3 \end{pmatrix},$$

where the theoretical mode shapes are dependent on amplitude.

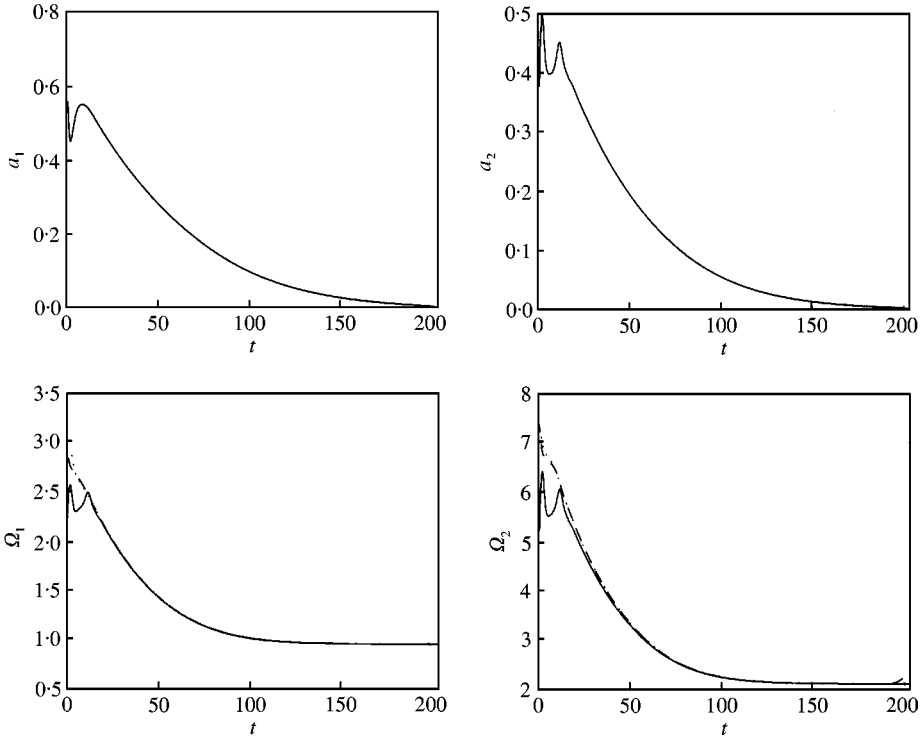

Figure 5. Example 1. Modal amplitudes extracted from x_1 and x_2. Non-linear modal frequencies (Ω_1 and Ω_2) versus time: extracted from x_1 (dashed lines), extracted from x_2 (dotted lines), theoretical (continuous lines).

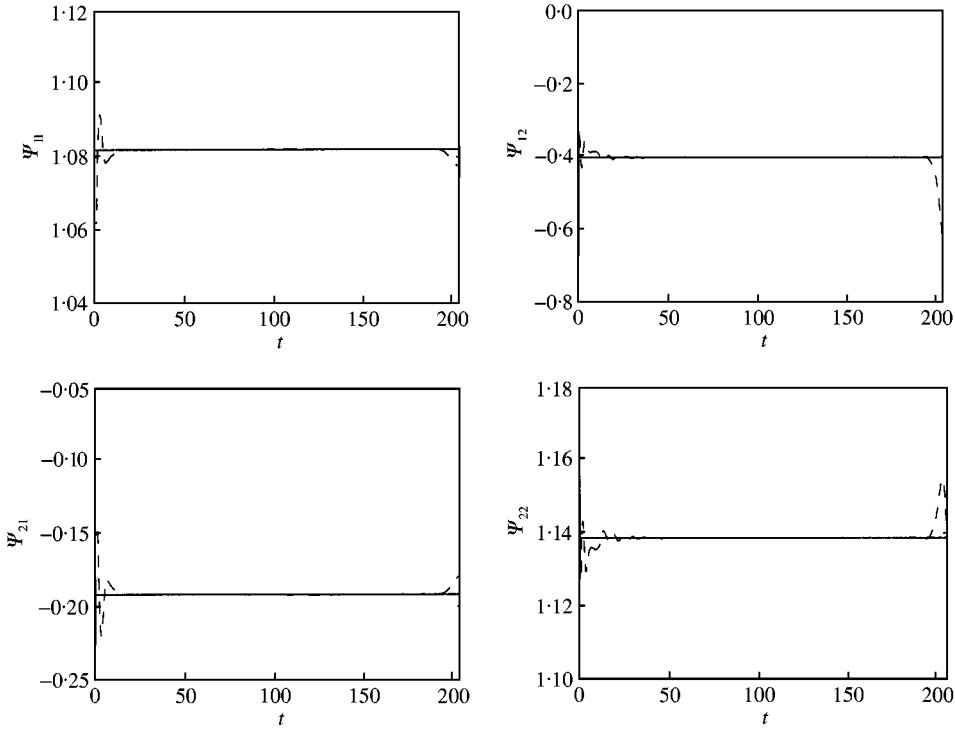

Figure 6. Example 1. Non-linear modal shapes versus time: extracted from x_1 and x_2 (dashed lines), theoretical (continuous lines).

Figure 7 shows the free response obtained with

$$X^0 = \begin{pmatrix} 0{\cdot}5 \\ 0{\cdot}5 \end{pmatrix}, \quad \dot{X}^0 = \begin{pmatrix} 0 \\ 0 \end{pmatrix}$$

used as the input data with the present method. All the results are given in Figures 8 and 9, which show the existence of good agreement between the theory and the estimate. This is an interesting example since it corresponds to a system in which the attenuation of each mode is different. This behaviour can be seen both in the signals themselves (Figure 7) and in the extracted modal amplitude components (Figure 8) which show that the second mode decreases faster than the first one. This provides an explanation for the behaviour of the extracted characteristics of the second mode component (see for example Ψ_{12} in Figure 9). Numerical instabilities actually appear when its amplitude becomes too small. Note also that the mode shape vector can be calculated up to a sign with this procedure (see Figure 9).

4.2. BEAM WITH ELASTIC STOPS

Considered here is a clamped-free beam with a pair of elastic stops fixed on the support (see Figure 10). The bending vibration of the beam with length L is governed by

$$\rho A \frac{\partial^2 u(z,t)}{\partial t^2} + \frac{\partial^2}{\partial z^2}\left(EI \frac{\partial^2 u(z,t)}{\partial z^2} \right) + h(u(z_b,t))\delta_0(z - z_b) = 0, \tag{43}$$

where EI, ρ, A, $u(z,t)$, $\delta_0(z)$ denote the stiffness bending, the mass density, the section area, the relative transversal displacement with respect to the frame at location z, and the Dirac

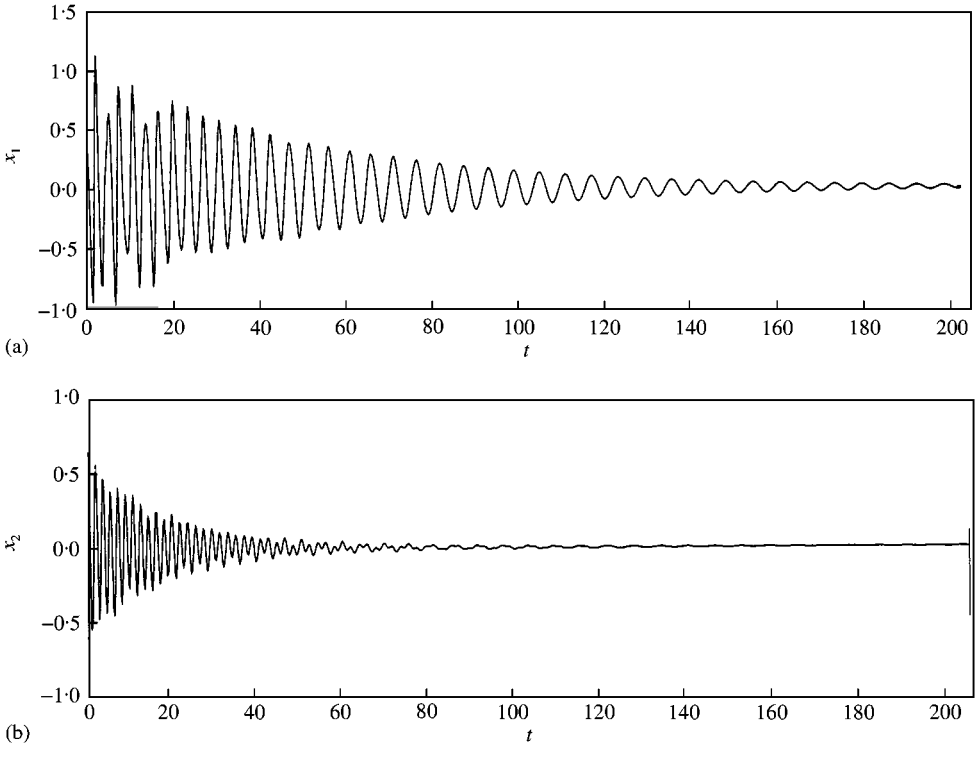

Figure 7. Example 2. Free oscillation.

delta function, respectively. The vibro-impact force at the impact location z_b is defined by

$$h(u) = \begin{cases} k_1(u - e_1), & e_1 < u \\ 0, & -e_2 < u < e_1 \\ k_2(u + e_2), & u < -e_2 \end{cases}, \tag{44}$$

where k_1 and k_2 denote the stiffnesses of the stops and e_1, e_2 the associated clearances.

By using the modal expansion principle, an approximate solution to equation (43) is given by

$$u_n(z, t) = \sum_{i=1}^{n} U_i(z) q_i(t), \tag{45}$$

where $U_i(z)$ denotes the mode shape associated with the natural frequency ω_i defining the ith mode of the linear nominal system (43) with $h(u) = 0$ (beam without stops).

The modal components $q_i(t)$ satisfy the non-linear differential equation

$$\ddot{q}_i(t) + 2\xi d_i \omega_i \dot{q}_i(t) + \omega_i^2 q_i(t) + \frac{U_i(z_b)}{\rho AL} h(u_n(z_b, t)) = 0 \quad \text{for } i = 1, \ldots, n. \tag{46}$$

These equations are coupled by non-linear terms and as usual, a viscous damping term has been added to account for the dissipative effects. Based on the approximation (45), and by using equation (46), the vector $X(t) = (u(z_1, t), \ldots, u(z_n, t))^{\mathrm{T}}$, which corresponds to the

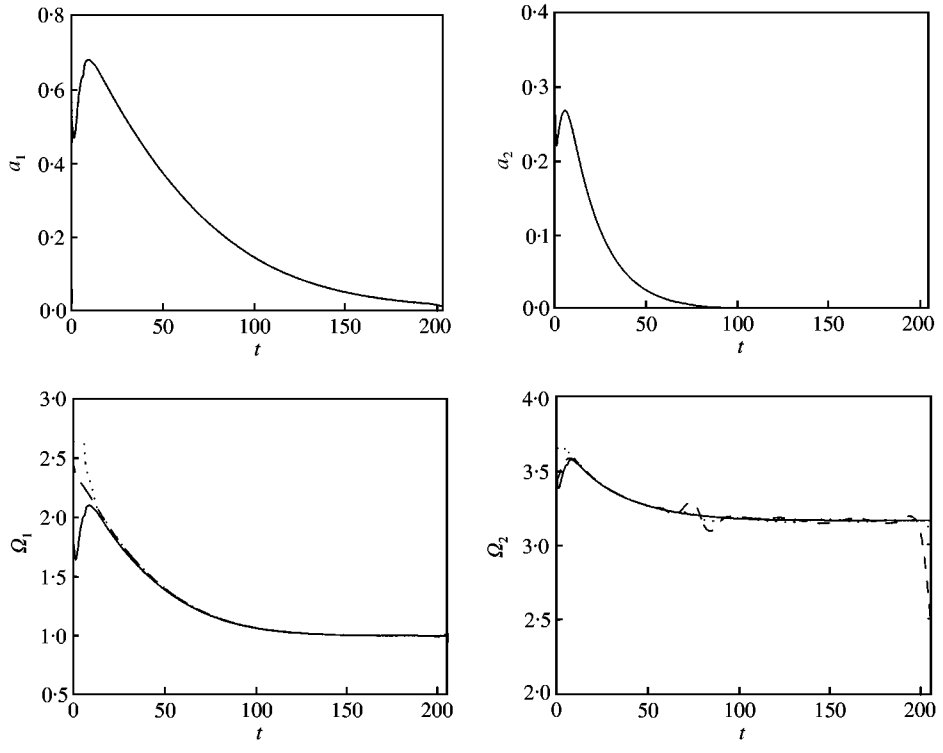

Figure 8. Example 2. Extracted modal amplitudes from x_1 and x_2. Non-linear modal frequencies (Ω_1 and Ω_2) versus time: extracted from x_1 (dashed lines), extracted from x_2 (dotted lines), theoretical (continuous lines).

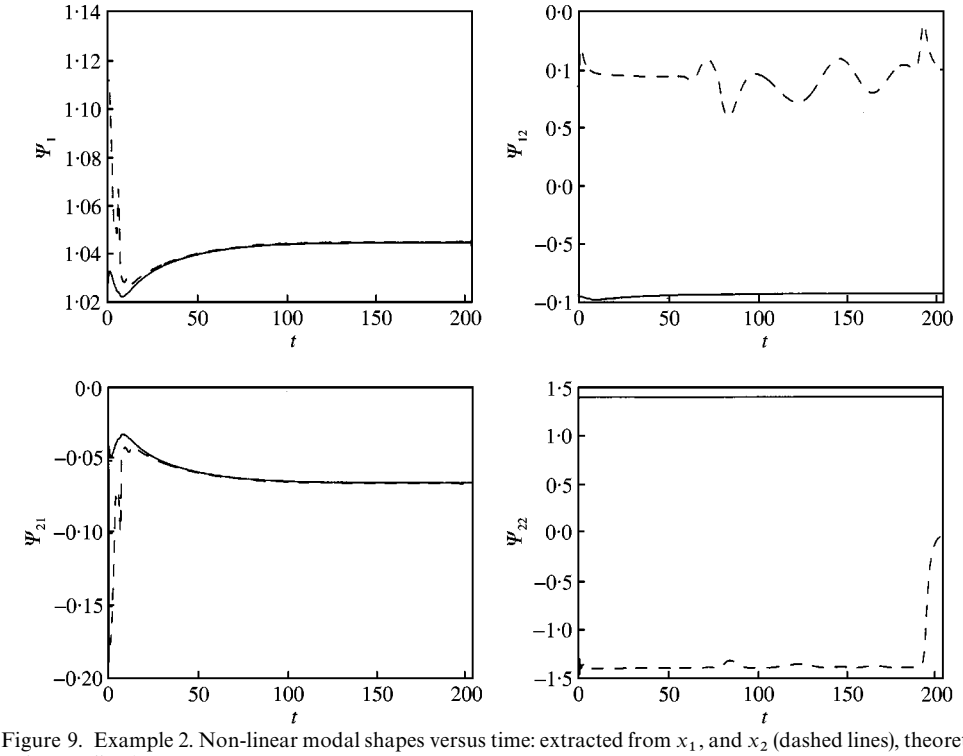

Figure 9. Example 2. Non-linear modal shapes versus time: extracted from x_1, and x_2 (dashed lines), theoretical (continuous lines).

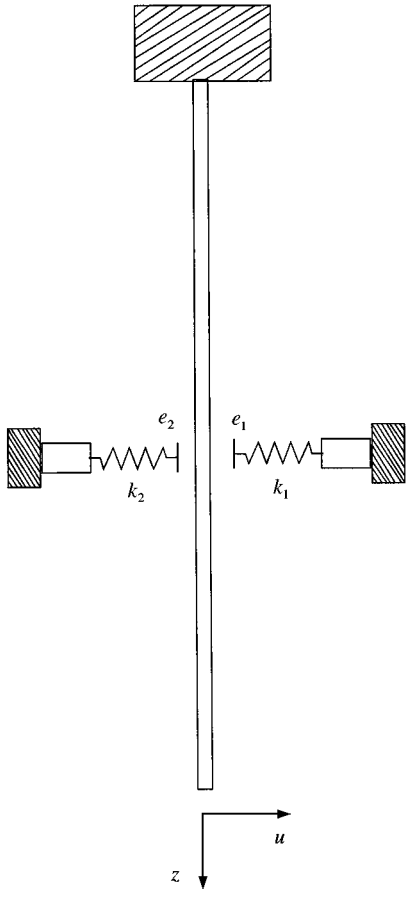

Figure 10. Beam with elastic stops.

deflection of the beam at n distinct points $z_1, \ldots, z_n$, can be characterized by a differential system of the form (1). This differential system has been studied here.

The simulation was performed with the parameter values of $EI = 326{\cdot}3\,\mathrm{N\,m^2}$, $\rho = 2495\,\mathrm{kg/m^3}$ (corresponding to an aluminium beam), and $L = 1\,\mathrm{m}$, $A = 1{\cdot}321 \times 10^{-4}\,\mathrm{m^2}$. The stops were placed at point $z_b = 0{\cdot}484\,\mathrm{m}$. The stiffnesses and (asymmetrical) clearance values were $k_1 = k_2 = 79107\,\mathrm{N/m}$, $e_1 = 0{\cdot}272 \times 10^{-3}\,\mathrm{m}$ and $e_2 = 0{\cdot}072 \times 10^{-3}\,\mathrm{m}$, respectively. Only two measurement points ($n = 2$, $z_1 = 0{\cdot}994\,\mathrm{m}$ and $z_2 = 0{\cdot}6\,\mathrm{m}$) have been taken into consideration, and hence only the first two modes were used in equation (45), where the natural frequencies of the associated linear system were $\omega_1/2\pi = 17{\cdot}5\,\mathrm{Hz}$ and $\omega_2/2\pi = 110\,\mathrm{Hz}$. The damping values chosen were $\xi = 0{\cdot}005$, $d_1 = 1$ and $d_2 = 1{\cdot}3$.

Figure 11 shows the free response ($u_1(t) = u(z_1, t)$ and $u_2(t) = u(z_2, t)$) at two points z_1 and z_2 used as input data with the method described above. All the results are given in Figures 12 and 13 and show the existence of good agreement between the theory and the estimate. Here the coupled non-linear modes have been defined by using the normalization procedure $\Psi_{ii}(a) = 1$ (see equations (6–8)). This is an interesting example, since it corresponds to an asymmetrical system leading to non-zero offset terms (see Figure 13). From the modal amplitude curves (see Figure 12), it can be seen that the decay times of the modal amplitudes are different and that the first mode dominates (in a ratio of 10). The

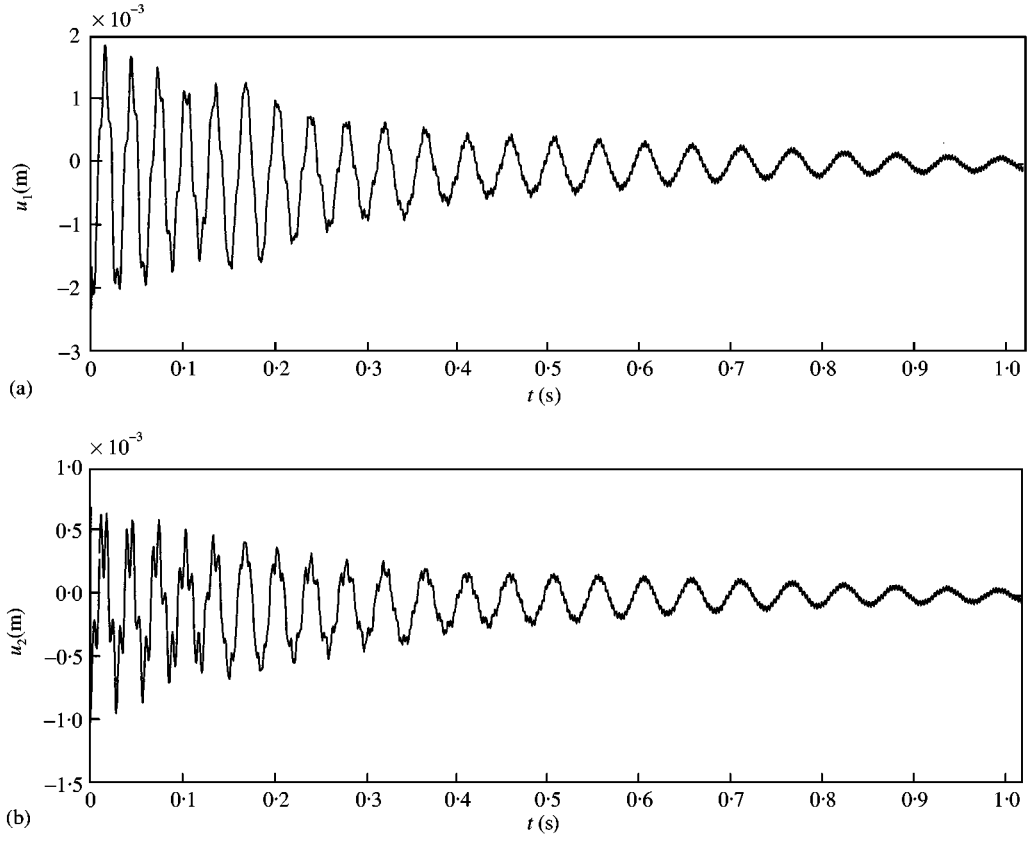

Figure 11. Beam with elastic stops. Free oscillation.

modal frequency of the first mode shows three different regions. The first one corresponds to a beam impacting both stops. The second one corresponds to a beam impacting only the nearest stop. The third one corresponds to the non-impacting case, in which the frequency is constant and corresponds to the natural frequency of the system: $\omega_1/2\pi = 17{\cdot}5$.

5. CONCLUSION

In this paper, a time–frequency domain method has been presented which can be used to identify the non-linear modal parameters of a multi-degree-of-freedom non-linear mechanical system. In particular, it was established that a time–frequency transformation of the transient response can be used to identify the non-linear modes. The advantage of time–frequency representations is that they make it possible to distinguish between the modal components of the same signal. In addition, an algorithm has been used with which each of the modal components can be continuously estimated. The good agreement existing between the extracted CNMs and the theoretical ones confirms the validity of the averaging principle as a means of characterizing the transient response by using the CNMs. In the examples given here, the bias introduced by the estimation procedure itself in the vicinity of the beginning of the signal does not mask the non-linear effect. However, in the case of systems which are strongly damped or show brief non-linear effects, for example, this bias

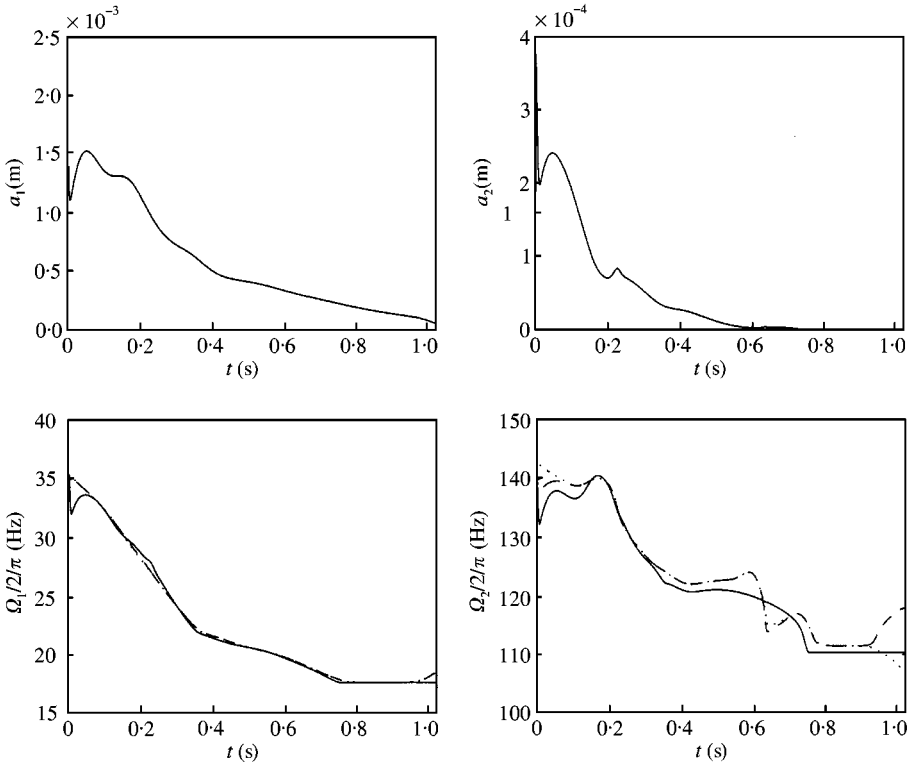

Figure 12. Beam with elastic stops. Modal amplitudes extracted from u_1 and u_2. Non-linear modal frequencies (Ω_1 and Ω_2) versus time: extracted from x_1 (dashed lines), extracted from x_2 (dotted lines), theoretical (continuous lines).

might be too large to give an accurate estimate. It is now proposed to develop procedures giving information about the damping. By using information available in the model, it should be possible to obtain a model for the frequency modulation law governing the elementary terms. This should make it possible to draw up and use a specific time–frequency representation that would give an exact estimate of the CNMs.

REFERENCES

1. D. J. EWINS 1995 *Modal Testing*: *Theory and Practice*. New York: Research Studies Press LTD, John Wiley Sons Inc.
2. R. M. ROSENBERG 1962 *Journal of Applied Mechanics* **29**, 7–14. The normal modes of nonlinear *n*-degree-of-freedom systems.
3. S. W. SHAW and C. PIERRE 1993 *Journal of Sound and Vibration* **164**, 85–124. Normal modes for nonlinear vibratory systems.
4. S. W. SHAW and C. PIERRE 1994 *Journal of Sound and Vibration* **169**, 319–347. Normal modes of vibration for nonlinear continuous systems.
5. A. F. VAKAKIS 1997 *Mechanical Systems and Signal Processing* **11**, 3–22. Nonlinear normal modes (NNMs) and their applications in vibration theory: an overview.
6. W. SZEMPLINSKA-STUPNICKA 1990 *The Behavior of Nonlinear Vibrating Systems*. Vol. I: *Fundamental Concepts and Methods*: *Applications to Single-Degree-of-Freedom Systems*, Vol. II: *Advanced Concepts and Applications to Multi-Degree-of-Freedom Systems*, volume 12 of *Mechanics*: *Dynamical Systems*. Dordrecht: Kluwer Academic Publishers.

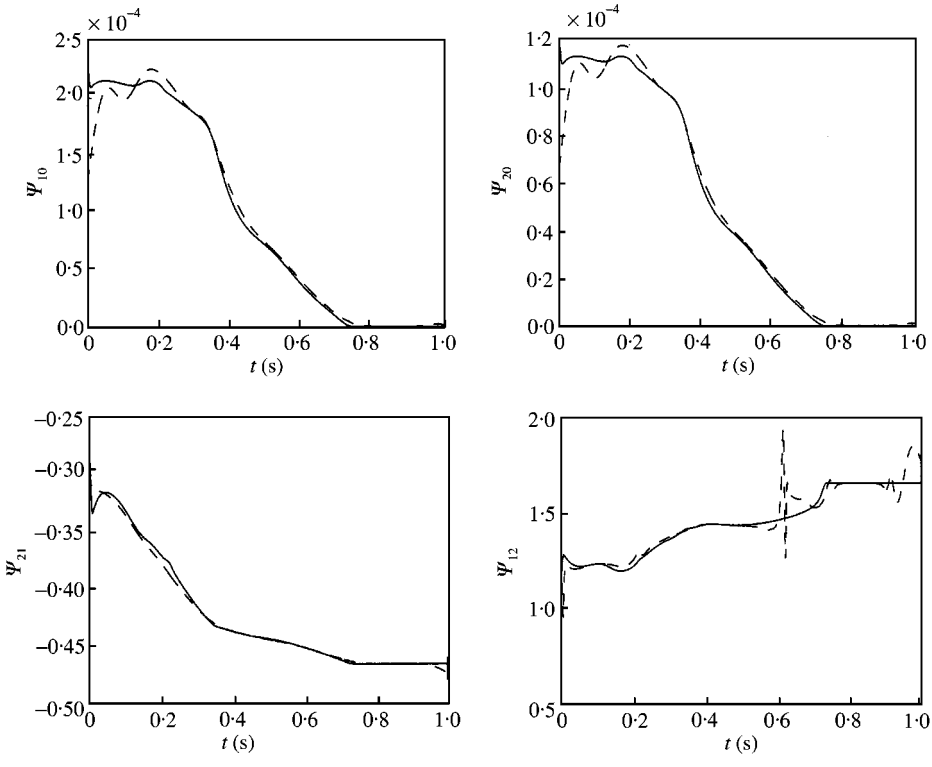

Figure 13. Beam with elastic stops. Offset terms (Ψ_0 and Ψ_{20}) and non-linear modal shapes: extracted from u_1, and u_2 (dashed lines), theoretical (continuous lines).

7. S. BELLIZZI and R. BOUC 1999 *Probabilistic Engineering Mechanics* **14**, 229–244. Analysis of multi-degree of freedom strongly nonlinear mechanical systems with random input. Part I: nonlinear modes and stochastic averaging.
8. S. BELLIZZI and R. BOUC 1999 *Probabilistic Engineering Mechanics* **14**, 245–256. Analysis of multi-degree of freedom strongly nonlinear mechanical systems with random input. Part II: equivalent linear system with random matrices and power spectral density matrix.
9. A. GROSSMANN, R. KRONLAND-MARTINET and J. MORLET 1989 *Wavelets, time-frequency methods and phase space*, 310–326. Berlin: Springer. in (C. A. Grossmann and P. Tchamitchian, editors), Reading and understanding continuous wavelet transform.
10. M. RUZZENE, A. FASANA, L. GARIBALDI and B. PIOMBO 1997 *Mechanical Systems and Signal Processing* **11**, 207–218. Natural frequencies and dampings identification using wavelet transform: application to real data.
11. W. J. STASZEWSKI 1997 *Journal of Sound and Vibration* **203**, 283–305. Identification of damping on MDOF systems using time-scale decomposition.
12. D. SPINA, C. VALENTE and G. R. TOMLINSON 1996 *Nonlinear Dynamics* **11**, 235–254. A new procedure for detecting nonlinearity from transient data using the Gabor transform.
13. L. GALLEANI, L. LOPRESTI and A. DESTEFANO 1998 *Signal Processing* **65**, 147–153. A method for non-linear system classification in the time frequency plane.
14. M. FELDMAN 1997 *Journal of Sound and Vibration* **208**, 475–489. Non-linear free vibration identification via the Hilbert transform.
15. W. J. STASZEWSKI 1998 *Journal of Sound and Vibration* **214**, 639–658. Identification of nonlinear systems using multi-scale ridges and skeletons of the wavelet transform.
16. F. VERHULST 1990 *Nonlinear Differential Equations and Dynamical Systems*. Berlin: Springer, Heidelberg.
17. J. C. RISSET 1965 *Journal of the Acoustical Society of America* **33**, 912–923. Computer study of trumpet tones.

18. D. GABOR 1946 *Journal of I.E.E.E.*, **93**, 429–441. Theory of communication.
19. A. GROSSMAN and J. MORLET 1984 *SIAM Journal of Mathematical Analysis* **15**, 723–736. Decomposition of hardy functions into square integrable wavelets of constant shape.
20. PH. GUILLEMAIN and R. KRONLAND-MARTINET 1996 *Proceedings of the IEEE, special issue on Wavelets* **84**(4), 561–585. Characterization of acoustic signals through continuous linear time–frequency representations.
21. N. DELPRAT, B. ESCUDIÉ, P. GUILLEMAIN, R. KRONLAND-MARTINET, P. TCHAMITCHIAN and B. TORRÉSANI 1992 *IEEE Transactions on Information Theory* **38**(2), 644–664. Asymptotic wavelet and Gabor analysis: extraction of instantaneous frequencies.

APPENDIX A: ALGORITHMIC ASPECT TO EXTRACT MODULATION LAWS

Consider the scalar signal

$$s(t) = \sum_{i=1}^{n} A_i(t) \cos(\Phi_i(t)), \quad t \in [0, T]$$

which is a combination of n simple elements with amplitude $A_i(t)$ and frequency modulation $\Phi_i'(t)$ laws. Denote by

$$L_g(\tau, s) = A_g(\tau, s) \mathrm{e}^{\mathrm{j}\Phi_g(\tau, s)}$$

the Gabor transform of $s(t)$. Under the asymptotic hypothesis for each simple element (see section 3.2), and by assuming that locally, the Gabor analysis deals only with one simple element, i.e. $\hat{W}(\Phi_i'(\tau) - \Phi_l'(\tau)) \simeq 0$, for $i \neq l$, the pairs $(\Phi_i'(\tau) - \Phi_k''(\tau))$ satisfy, for $i = 1, \ldots, n$ and for all $\tau \in [0, T]$, the so-called crossed criterion

$$\left(\frac{\partial}{\partial\tau} + \Phi_i''(\tau)\frac{\partial}{\partial\alpha}\right)\Phi_g(\tau, \Phi_i'(\tau)) = \Phi_i'(\tau),$$

$$\left(\frac{\partial}{\partial\tau} + \Phi_i''(\tau)\frac{\partial}{\partial\alpha}\right)^2 \Phi_g(\tau, \Phi_i'(\tau)) = \Phi_i''(\tau).$$

The set of points $(\tau, \Phi_i'(\tau))$ with $\tau \in [0, T]$ defines the ridge of the ith simple element.

In order to extract for each simple element the frequency modulation law $\Phi_i'(\tau)$ (leading to $\Phi_i(\tau)$ and $A_i(\tau)$ from equations (35) and (36)), a continuation method combined with the classical fixed-point algorithm is used to solve with respect to (α, β) the algebraic systems

$$\left(\frac{\partial}{\partial\tau} + \beta\frac{\partial}{\partial\alpha}\right)\Phi_g(\tau, \alpha) = \alpha, \quad \left(\frac{\partial}{\partial\tau} + \beta\frac{\partial}{\partial\alpha}\right)^2 \Phi_g(\tau, \alpha) = \beta,$$

for τ varying in $[0, T]$.

For a given time $\tau_k \in [0, T]$, the fixed point algorithm with the two variables α and β is as follows.

- Update step.

$$\alpha_{l+1} = \frac{\partial\Phi_g(\tau_k, \alpha_l)}{\partial\tau} + \beta_l \frac{\partial\Phi_g(\tau_k, \alpha_l)}{\partial\alpha},$$

$$\beta_{l+1} = \frac{\partial}{\partial\tau}\left(\frac{\partial\Phi_g(\tau_k, \alpha_l)}{\partial\tau} + \beta_l\frac{\partial\Phi_g(\tau_k, \alpha_l)}{\partial\alpha}\right) + \beta_l\frac{\partial}{\partial\alpha}\left(\frac{\partial\Phi_g(\tau_k, \alpha_l)}{\partial\tau} + \beta_l\frac{\partial\Phi_g(\tau_k, \alpha_l)}{\partial\alpha}\right).$$

This expression for β_{l+1} is numerically easy to compute, since it can be viewed as the difference between two α_{l+1} values computed at two different frequencies (the difference between which is β_l) and two consecutive samples. The two α_{l+1} values are obtained by deriving the phase of the transform between two consecutive samples at two different frequencies (the difference between which is also β_l).

- Convergence criteria. With $\forall\varepsilon$ taken to be arbitrarily small, the criteria are

$$|\alpha_{l+1} - \alpha_l| < \varepsilon, \quad |\beta_{l+1} - \beta_l| < \varepsilon.$$

By assuming $\beta = \Phi_r''(\tau_k)$, one can prove the convergence of the algorithm giving α. The convergence of the algorithm which gives β has been checked only numerically.

The choice of the initial values to start the fixed point algorithm depends on the value of the time τ. Two cases have to be considered.

- For $k = 0$ (i.e. $\tau_0 = 0$), the initial values α_0 and β_0 fix the ridge to follow. In practice, the value α_0 is obtained from the local maximum of the modulus of the Gabor transform near $\tau_0 = 0$ and $\beta_0 = 0$.
- The continuation process from time τ_k to time $\tau_{k+1} = \tau_k + \mathrm{d}\tau$ is performed with initial values

$$\alpha_0 = \alpha_\infty + \beta_\infty \,\mathrm{d}\tau, \quad \beta_0 = \beta_\infty,$$

where α_∞ and β_∞ denote the values of α and β obtained when the convergence criteria are satisfied for the time τ_k.